sustainability

MDPI

Article

Unit Commitment Considering Electric Vehicles and Renewable Energy Integration—A CMAES Approach

Qun Niu [1,*], Lipeng Tang [1], Litao Yu [1], Han Wang [1] and Zhile Yang [2]

[1] Shanghai Key Laboratory of Power Station Automation Technology, School of Mechanical Engineering and Automation, Shanghai University, Shanghai 200444, China
[2] Shenzhen Institute of Advanced Technology, Chinese Academy of Sciences, Shenzhen 518055, China; zl.yang@siat.ac.cn
* Correspondence: nq@shu.edu.cn

Abstract: Global fossil fuel consumption and associated emissions are continuing to increase amid the 2022 energy crisis and environmental pollution and climate change issues are becoming even severer. Aiming at energy saving and emission reduction, in this paper, a new unit commitment model considering electric vehicles and renewable energy integration is established, taking into account the prediction errors of emissions from thermal units and renewable power generations. Furthermore, a new binary CMAES, dubbed BCMAES, which uses a signal function to map sampled individuals is proposed and compared with eight other mapping functions. The proposed model and the BCMAES algorithm are then applied in simulation studies on IEEE 10- and IEEE 118-bus systems, and compared with other popular algorithms such as BPSO, NSGAII, and HS. The results confirm that the proposed BCMAES algorithm outperforms other algorithms for large-scale mixed integer optimization problems with over 1000 dimensions, achieving a more than 1% cost reduction. It is further shown that the use of V2G energy transfer and the integration of renewable energy can significantly reduce both the operation costs and emissions by 5.57% and 13.71%, respectively.

Keywords: unit commitment; electric vehicles; renewable generation; emission reduction; binary covariance matrix adaption evolution strategy

Citation: Niu, Q.; Tang, L.; Yu, L.; Wang, H.; Yang, Z. Unit Commitment Considering Electric Vehicles and Renewable Energy Integration—A CMAES Approach. *Sustainability* **2024**, *16*, 1019. https://doi.org/10.3390/su16031019

Academic Editors: Yiji Lu, Miltiadis (Miltos) Alamaniotis, Nicoletta Matera, Kangli Liu and Na Chai

Received: 12 October 2023
Revised: 13 January 2024
Accepted: 17 January 2024
Published: 25 January 2024

1. Introduction

In light of the energy crisis of the new century, rethinking power generation in power systems is becoming increasingly popular. Traditional thermal power plants mainly rely on fossil fuels to generate electricity. The substantive consumption of fossil fuels and the subsequent emissions have been identified as one of the main contributors to climate change and the deterioration in air quality, particularly, in the midst of the energy crisis in 2022. To address these global challenges, the large scale roll-outs of renewable energy and electric vehicles are viewed as important measures. The integration of renewable energy and electric vehicles into the grid can reduce both operation costs and capital costs in building more power system assets, while effectively reducing greenhouse gas emissions. It is estimated that by 2030, carbon dioxide emissions will be reduced by up to 77.6 million tons and environmental costs will be reduced by up to USD 18.945 billion [1]. However, due to the uncertainty in and volatility of renewable energy, balancing supply and demand in the power grid become more difficult, and brings significant challenges to the unit scheduling, power grid control, and market operation of power systems [2]. Therefore, it is of great significance to study the impact of renewable energy and electric vehicles on a power grid to reduce the operating costs while maintaining its stable operation.

The unit commitment (UC) problem is an NP-hard combinatorial optimization problem of high dimension and strong nonlinearity subject to multiple constraints. Reasonable allocation of the generated power of the unit can bring forward tangible economic benefits to the power system and ensure its safe and stable operation. The unit

commitment problem was first discussed in 1966. Under the premise of stable operation of the power generation units, the start-stop planning of the unit and its output power are allocated in unit time, to minimize the operating cost of the whole system. The traditional thermal power unit model has been widely studied. Generally, approaches to consider the integration of intermittent renewable energy in the UC problem can be divided into two types [3]. The first approach is to develop a stochastic model for renewable generation units, while the second approach is to formulate a deterministic UC problem.

Among these approaches, the deterministic method is more commonly used, and a range of techniques have been proposed to evaluate the impact of EVs or RE on the power system UC problem. In a 2010 study [4], a model considering only one electric vehicle (EV) charging mode was incorporated, which can significantly reduce both the cost and emissions of the unit. A 2014 study [5] designed a UC model with electric vehicles as flexible loads and the cost is increased by charging electric vehicles. These approaches are useful for studying the impact of electric vehicles on the grid, but they only consider one operating mode of electric vehicles. Ehsan et al. [6] evaluated the V2G and G2V modes in the UC of the power system. The simulation results show that both the cost and spinning reserve can be reduced but it does not consider renewable energy. A 2012 study [7] proposed a UC with a spinning reserve for a microgrid with solar and wind energy storage and considered the prediction error of wind speed and solar radiation of the system. However, the impact of EVs on the power system is not analyzed. Two further studies [2,8] designed three models for UC, EV, and RE, respectively, in the UC problem, but the approach mainly considered the influence of RE and EVs on the system, while the prediction error of RE on the spinning reserve requirement was not discussed. To produce reliable and cost-effective UC, it is vital to consider the influence of EV integration and RE intermittency on the UC problem of the power systems. A schematic diagram to illustrate the UC considering electric vehicles and renewable energy is given in Figure 1.

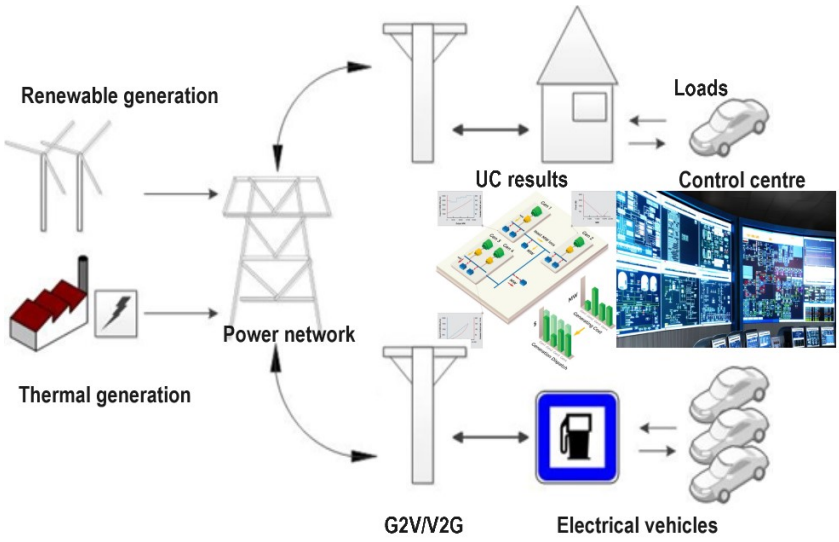

Figure 1. Schematic diagram of the unit commitment considering electric vehicles and renewable energy.

As a conventional NP-hard problem, the UC problem has the characteristics of strong nonlinearity, large scale, mixed integer, and high dimension. Some traditional mathematical methods were first used to solve this problem, such as Dynamic Programming (DP), Integer Programming (IP), Mixed-integer Programming (MIP), Branch and Bound Methods (BBM), and Lagrangian Relaxation (LR) [9]. Although these traditional methods can achieve good results for a limited number of problems, as the model complexity and system scale increases, traditional mathematical methods may encounter the dimensionality problem and the quality and reliability of the resulting solutions may be greatly reduced.

Intelligent optimization algorithms emerged in the 1980s and among the first was the Genetic Algorithm (GA) proposed by Holland based on Darwin's "survival of the fittest"

biological evolution law. Other popular methods have also been proposed in the last few decades. For example, the simulated annealing algorithm proposed by Kirkpatrick et al. based on the principle of slow annealing of solids in physics, Particle Swarm Optimization (PSO) proposed by Kennedy and Eberhart, which was inspired by observing the phenomenon of bird foraging. Similarly, Storn and Price proposed the Differential Algorithm (DE), which is a probability-based algorithm, by simulating the mutual cooperation and competition between individuals. The Ant Colony Algorithm (ACO) proposed by Dorigo and Stützle, based on the process of finding the optimal path when ants carry food, is a probabilistic algorithm for finding the shortest path. The Shuffled Frog Leaping Algorithm (SFLA) proposed by Eusuff and Lansey imitates the behavior of frogs interacting with each other during foraging, while Basturk and Karaboga proposed an artificial bee colony algorithm by observing and imitating the behavior of bees. In recent years, with the further development of computer technology and artificial intelligence, many new intelligent optimization algorithms have been introduced. For example, the Harmony Search Algorithm (HS) [10], Teaching-and-Learning-based Optimization (TLBO) [11], and the Quantum-inspired Algorithm (QEA) [12]. These heuristic algorithms can be more flexible and more adaptive in solving UC problems; however, although many methods have been proposed to solve the UC problem, the quality and efficiency of solutions for high-dimensional UC problems still have much room for improvement.

The Covariance Matrix Adaption Evolution Strategy (CMAES) is an evolutionary method proposed by Hansen et al. that continuously adjusts the covariance matrix of its multidimensional normal distribution during evolution [13]. The CMAES algorithm mainly uses a rank 1 update to ensure contemporary information, and a rank μ update to ensure the relationship between generations. It avoids falling into local optima unlike other algorithms such as the Genetic Algorithm (GA) and Particle Swarm Optimization (PSO), and has the advantages of strong robustness and optimization capability. Improved CMAES methods have also been proposed. For example, an orthogonal CMAES [14] was proposed to incorporate a quantitative orthogonal design to address the high-dimensional premature convergence problem of the conventional CMAES algorithm. In order to solve large-scale real-valued optimization problems, the partition strategy was also introduced to the CMAES algorithm in a 2012 study [15].

The CMAES algorithm has been widely used in various fields, such as the design of materials, electrical systems, control engineering, and scientific computing. For example, Manoharan used the CMAES algorithm to solve the dynamic economic load problem [16]. Salman et al. proposed to combine the CMAES and DE algorithms for the optimal design of reinforced concrete structures [17]. Jia proposed the BESS Covariance Matrix Adaptation Evolution Strategy (CMA-ES) dispatch algorithm to optimal Hybrid Renewable Energy Systems. Jia proposed a CMAES algorithm for global optimization of large-scale overlapping problems [18]. Rezk et al. used the CAMES algorithm to design horn ripples [19]. Raufet al. used the CMAES algorithm to determine the parameters of a traditional wind-power optimization algorithm [20].

It should be noted that the CMAES algorithm has been mainly used for solving continuous optimization problem, while little has been done for discrete systems. Aiming to address the limitations of CMAES, this paper proposes a new Binary Covariance Matrix Adaption Evolution Strategy (BCMAES) algorithm, which is used to solve the binary optimization problem, and applies the algorithm to solve the UC problem, which is often a nonlinear large-scale mixed integer optimization problem.

The highlights and the main contributions of this paper are summarized below.

- A new discrete mapping operator is designed and compared with eight popular mapping operators. This new operator allows the CMAES to become applicable to solving discrete optimization problems;
- The discrete CMAES method is applied to large-scale UC problems for the first time;

- Two different test systems consisting of 10- and 54-unit power networks are tested in order to evaluate the searching capability of the proposed algorithm in test cases of different scales, achieving operating costs reduction of 1.92% and 1.13%, respectively;
- The elite reservation strategy and restart strategy are adopted to strengthen the global search capability of the algorithm and achieve population adaptation.

The remainder of the paper is organized as follows: Section 2 presents the formulation of the unit commitment problem, while the proposed Binary Covariance Matrix Adaption Evolution Strategy (BCMAES) algorithm is presented in Section 3 and its implementation for a UC problem is presented in Section 4. The numerical results and analysis are given in Section 5. Finally, Section 6 concludes the paper.

2. Problem Formulation

The unit commitment problem considered in this paper includes three models: the basic unit commitment problem, the UC problem considering electric vehicles, and the UC problem considering both electric vehicles and renewable energy.

2.1. Unit Commitment Problem with Electric Vehicles

Charging and Discharge Mode of Electric Vehicle

With the further development of EV technology, Kempton et al. proposed in 1997 [21] that electric vehicles can be used as mobile energy storage devices, i.e., in addition to receiving electricity from the grid, they can also release electricity to the grid. This discharge process from electric vehicles to the grid is called V2G (Vehicle to Grid). The discharge modes of electric vehicles are discussed below [22].

With the development of smart grid technology, four typical coordinated control modes of electric vehicle charging have emerged. They are the Electric Power Research Institute Charging Model (EPRICM), the Off-peak Charging Model (OPCM), the Peak Charging Model (PCM), and the Stochastic Charging Model (SCM) [22].

Considering the uncertainty in the driver's charging behavior, a random charging curve SCM is proposed. The unexpected load curve simulates some emergency group charging or distributed fast charging at random times throughout the day. The random probability follows a normal distribution with an average of 5%. The probability of random charging distribution per hour is 1.1% to 9.7%. The charging probability will change randomly regardless of the peak or off-peak load time.

- Objective function

  The Unit Commitment with Electric Vehicles (UCEV) problem model is adapted from the basic UC problem model. Its objective function is similar to that of the fundamental UC problem, but the constraints are different. The objective function of the UCEV problem is given in Equation (1):

$$\min F^{UCEV} = \sum_{t=1}^{T} \sum_{i=1}^{N} [F_{FC,i} + F_{SC,i}(1 - U_i(t-1))]U_i(t) \quad (1)$$

  When the objective function considers emissions, Equation (1) can be rewritten as follows:

$$\min F^{UCEV} = \sum_{t=1}^{T} \sum_{i=1}^{N} [\varphi_c(F_{FC,i} + F_{SC,i}(1 - U_i(t-1))) + \varphi_e F_{em,i}]U_i(t) \quad (2)$$

  In this objective function, the cost of the electric vehicle is neglected. The model uses two quadratic cost functions. In addition to the fuel cost of the basic UC problem, the emission cost is also considered. In Equation (3), $F_{em,i}$ is the emission target, and its quadratic function unit power generation is as follows:

$$F_{em,i} = \alpha_i + \beta_i P_{u,i}(t) + \gamma_i(P_{u,i}(t)) \quad (3)$$

where a_i, b_i, and c_i are the weight coefficients of cost and emission, respectively;

- Units Constraints

The constraint conditions have also significantly changed, mainly in terms of the power balance and spinning reserve constraints. Some constraints of the electric vehicle itself, the load capacity constraint of the electric vehicle, the balance constraint of the electric vehicle, and the battery capacity balance constraint, are also added.

The uncertain power output from the EVs and the output from the thermal power units must meet the load demand, as defined below:

$$\sum_{i=1}^{N} P_{u,i}(t)U_i(t) + P_c(t) = P_d(t) \tag{4}$$

The power output from the electric vehicles can be calculated as follows:

$$P_c(t) = N_{EV}(t) \times PV_{av} \times \eta_{EV} \times \delta \tag{5}$$

where $P_c(t)$ is the total efficiency of the electric vehicles, $N_{EV}(t)$ represents the number of electric vehicles integrated into the grid at time t, PV_{av} is the average battery capacity of an electric vehicle, and σ presents the average percentage of batteries that electric vehicles need to charge.

For reliable operation, the spinning reserve needs to be constrained as follows:

$$\sum_{i=1}^{N} P_{u,i}^{\max} U_i(t) + P_{c,\max}(t) >= Pd(t) \times (1 + SR) \tag{6}$$

The maximum power output of the electric vehicle at time t. $P_{c,max}(t)$ can be obtained by the following equation:

$$P_{c,\max}(t) = N_{EV}(t) \times PV_{\max} \times \eta_{EV} \times \delta \tag{7}$$

The PV_{max} represents the maximum battery capacity of the electric vehicle;

- Electric vehicle constraints

Load capacity limitation of electric vehicles The power supply connected to the grid is limited by the capacity of the interface in the parking base area, as given below:

$$N_{EV}^{\min}(t) \leq N_{EV}(t) \leq N_{EV}^{\max}(t) \tag{8}$$

Balance constraint of electric vehicle. The number of electric vehicles registered on the grid within a day is fixed, and all-electric vehicles connected to the grid must meet the following constraints:

$$\sum_{t=1}^{T} N_{EV}(t) = N_{EV}^{\text{total}} \tag{9}$$

Battery power balance. For the V2G/G2V mode of the electric vehicles, the charging capacity and discharge capacity of the battery must be limited by the balance of battery power, which can be expressed as follows:

$$\sum_{t_1=1}^{T_1} N_{EV}^{G2V}(t) = \sum_{t_2=1}^{T_2} N_{EV}^{V2G}(t) \tag{10}$$

where T_1 and T_2 are the time periods for the electric vehicles to charge and discharge, respectively, and $N_{EV}^{G2V}(t)$ and $N_{EV}^{V2G}(t)$ are the number of electric vehicles charging/discharging to the grid at time t, respectively.

2.2. Unit Commitment Problem with Electric Vehicles and Renewable Energy

2.2.1. Mathematical Model of UC Problem with Electric Vehicles and Renewable Energy

- Objective function
  The model for the Unit Commitment with Electric Vehicles and Renewable Energy (UCEVR) problem is a more complex model based on UCEV. The UCEVR objective function is exactly the same as the UCEV objective function. These renewable energy sources do not affect the change in the model objective function, as shown below:

$$\min F^{UCEVR} = \sum_{i=1}^{T}\sum_{i=1}^{N}\left[\varphi_c\left(F_{fc,i} + F_{sc,i}(1 - U_i(t-1))\right) + \varphi_e F_{em.i}\right]U_i^{(t)} \tag{11}$$

- Units Constraints
  The UCEVR model is based on the UCEV model. For the constraints, the original power-balance conditions and spinning reserve constraints are changed. Equations (12) and (13) have changed as follows:

$$\sum_{i=1}^{N} P_{u,i}(t)U_i(t) + P_w(t) + P_s(t) + P_c(t) = P_d(t) \tag{12}$$

$$\sum_{i=1}^{N} P_{u,i}^{\max}U_i(t) + \eta_R(P_w(t) + P_s(t)) + P_{c,\max}(t) >= Pd(t).(1 + SR) \tag{13}$$

  where η_R is the prediction error of renewable energy because the renewable energy in the model is mainly composed of wind and solar energy. So, $P_w(t)$ and $P_s(t)$ represent the output power of wind energy and solar energy at time t, respectively;
- Renewable energy constraints
  Renewable energy has the feature of being unpredictable. Hence, we will only use a portion of the predicted power of renewable energy for power system scheduling. Especially when it comes to the constraints of spinning reserves, we need to consider the prediction error of renewable energy.

2.2.2. Prediction of Renewable Energy

Wind and solar energies are considered in the mathematical model of UCEVR. The predicted solar data are collected from the literature [4,8]. These data are given in Table 1:

Table 1. The expected value of the predicted solar and wind power generation.

time (h)	1	2	3	4	5	6	7	8
solar (MW)	0	0	0	0	0	0	0.09	17.46
wind (MW)	44	70.2	76	82	84	84	100	100
time (h)	9	10	11	12	13	14	15	16
solar (MW)	31.45	36.01	38.06	35.93	36.78	31.59	9.7	12.92
wind (MW)	78	64	100	92	84	80	78	32
time (h)	17	18	19	20	21	22	23	24
solar (MW)	0	0	0	0	0	0	0	0
wind (MW)	4	8	10	5	6	56	82	52

Three thousand wind power scenarios were generated within 24 h usingatin hypercube sampling to simulate wind fluctuations. This paper reduces the number of scenarios to 10 using scenario-reduction techniques [23]. The final wind energy is shown in Figure 2, and the corresponding probability is shown in Table 2.

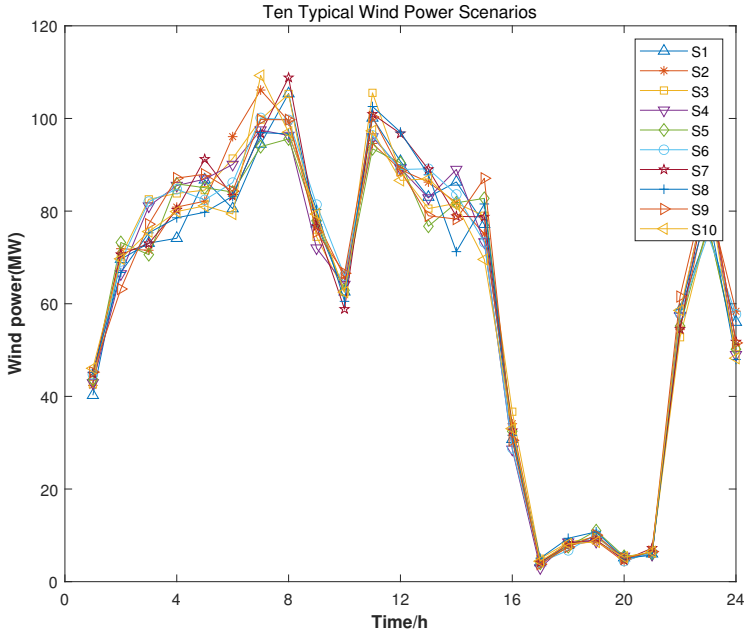

Figure 2. Ten wind energy scenarios.

Table 2. The probability for each of the 10 wind power generation scenarios.

Scenario	1	2	3	4	5	6	7	8	9	10
possibility	0.123	0.089	0.072	0.056	0.166	0.077	0.141	0.13	0.093	0.056

To select a representative wind energy fluctuation scenario, a performance index is introduced, consisting of target cost and wind power supply security calculations [24], which is defined as follows:

$$Index_1(s) = \frac{F_{fc}^s + F_{sc}^s + F_{ec}^s}{\sum_{i=1}^{10} \left(F_{fc}^i + F_{sc}^i + F_{ec}^i \right)} \tag{14}$$

$$Index_2(s) = \frac{1}{T} \sum_{i=1}^{T} \frac{P_w^s(t)}{\sum_{i=1}^{10} P_w^i(t)} \tag{15}$$

$$Sec(s) = \frac{ps}{(Index_1(s) + Index_2(s))} \tag{16}$$

where $Index_1$ is the target cost of the power system, $Index_2$ is the wind energy security value of the power system when selecting the sth wind energy scenario, and ps is the probability value of the sth wind energy scenario. Sec is the probability of the performance index. We will need to select the wind power generation scenario with the highest Sec as the representative wind power generation scenario.

3. Binary Covariance Matrix Adaptation Evolution Strategy

3.1. Covariance Matrix Adaptation Evolution Strategy

The CMAES algorithm is a continuous optimization algorithm proposed by Hansen in 2003 [13] that generates new population individuals by sampling from the probability distribution constructed in the optimization process. The CMAES algorithm is derived from the adaptive concept in evolutionary strategy, which adapts to the covariance matrix of a multivariate normal distribution. One of the core concepts of the algorithm is to

learn the correlation of parameters and use this correlation to accelerate the convergence of the algorithm. Due to this learning process, the CMAES algorithm performs a search independently of the coordinate system, reliably adapts to the topology of any function, and significantly improves the convergence speed, especially on objective functions that are inseparable or have a poor scaling ratio.

For nonlinear optimization such as non-convex or rough search environments (such as sharp bending, discontinuity, outliers, noise, and local optimum), CMAES is a better choice than classical optimization methods (such as the quasi-Newton method or conjugate gradient method). Learning the covariance matrix in CMAES is similar to learning the inverse Hessian matrix in the quasi-Newton method. The update of the covariance matrix makes the search distribution adapt to the problem of poor scaling ratio and non-separability so that CMAES can overcome the limitations of the typical evolutionary algorithms in solving such issues.

A typical reason for the failure of population-based search algorithms is that complex methods degrade the population into subspaces. This is usually prevented by non-adaptive components in the algorithm or a large population size (much larger than the dimension of the problem). In the CMAES algorithm, the population size can be freely selected because the learning rate of the covariance matrix C_μ can prevent degradation. At the same time, use of step size control can avoid the premature convergence of the population.

3.2. Binary Adaptive Matrix Covariance Evolution Strategy

Many practical problems can be formulated as discrete binary optimization problems, such as the knapsack problem, renewable power generation location problem, and path planning problem, to name a few. These problems are NP-hard problems, and their main difficulty lies in the fact that the search space will exhibit an exponential growth trend with the increase in the number of dimensions. This type of problem also often has the characteristics of non-convexity, nonlinearity, and non-differentiability, and there is very little mathematical information that can be utilized. Classical optimization methods are no longer competent. Therefore, intelligent optimization algorithms are a good choice. The binary particle swarm optimization algorithm limits the position of the individual to between 0 and 1 by rewriting the position update formula of the algorithm [25]. The binary firefly algorithm discretizes the algorithm by redefining the displacement formula of the firefly by binary coding the individual fireflies [26]. The binary differential evolution algorithm without parameter mutation can directly mutate in the discrete domain via the difference between individuals [27]. CMAES is an effective optimization method for solving continuous optimization problems. It performs well in solving continuous multimodal standard test functions, but the algorithm is not suitable for binary optimization problems. Aiming at the limitations of the CMAES algorithm, this paper proposes a binary covariance matrix adaptive evolution strategy, and applies the CMAES algorithm to the field of binary problems.

3.2.1. Variable Discretization

The rounding method can discretize continuous variables into binary variables. Since the CMAES algorithm generates a solution space subject to a normal distribution through Gaussian variation, we can discretize the constant variables of the solution space into binary variables by rounding. According to a 2006 study [28], the initial search points are randomly distributed between [0, 1]. The initial step size is set to five to ensure that the initial search points are distributed between 0 and 1. A new set of solutions is generated through an algorithm update, and then the new solutions are binary-coded by the following rounding function.

$$x_k^{(g+1)} = \begin{cases} 0, & \text{if} \quad 0 \le x_k^{(g+1)} < 0.5 \\ 1, & \text{if} \quad 0.5 \le x_k^{(g+1)} < 1 \end{cases} \tag{17}$$

It should be noted that in the process of continuous convergence of the entire algorithm, it is likely that some solutions will cross the boundary. Here, we usually adopt a general boundary treatment strategy, that is, the endpoint value method, as shown below:

$$x_k^{(g+1)} = \begin{cases} 0, & \text{if} \quad x_k^{(g+1)} < 0 \\ 1, & \text{if} \quad x_k^{(g+1)} > 1 \end{cases} \tag{18}$$

Therefore, we can combine the above two equations, yielding:

$$x_k^{(g+1)} = \begin{cases} 0, & \text{if} \quad x_k^{(g+1)} < 0.5 \\ 1, & \text{if} \quad x_k^{(g+1)} > 0.5 \end{cases} \tag{19}$$

In this way, we have initially achieved the goal of simply discretizing population individuals. In order to better validate the effectiveness of the above discrete methods, we also selected the discrete design method from a 2013 study [29] as shown in Table 3, and compared it with the above discrete methods. In summary, we use eight different transfer functions as variable discretization, as shown in Table 3. Four are S-type, and the other four are V-type. The shapes of the nine transfer functions are shown in Figure 3.

Table 3. Different discretization methods.

Binary Symmetric Particle Swarm Optimization Family	
Name	**Transfer Function**
BCMAES1	$T(x) = \frac{1}{1+e^{-2x}}$
BCMAES2	$T(x) = \frac{1}{1+e^{-x}}$ a
BCMAES3	$T(x) = \frac{1}{1+e^{(-1/2x)}}$
BCMAES4	$T(x) = \frac{1}{1+e^{(-1/3x)}}$
BCMAES5	$T(x) = \lvert \operatorname{erf}\left(\frac{\sqrt{\pi}}{2}x\right) \rvert = \lvert \frac{\sqrt{2}}{\pi} \int_0^{(\sqrt{\pi}/2)x} e^{-t^2} dt \rvert$
BCMAES6	$T(x) = \lvert \tanh(x) \rvert$
BCMAES7	$T(x) = \left\lvert (x)/\sqrt{1+x^2} \right\rvert$
BCMAES8	$T(x) = \left\lvert \frac{2}{\pi} \arctan\left(\frac{\pi}{2}x\right) \right\rvert$
BCMAES9	$T(x) = x < 0$

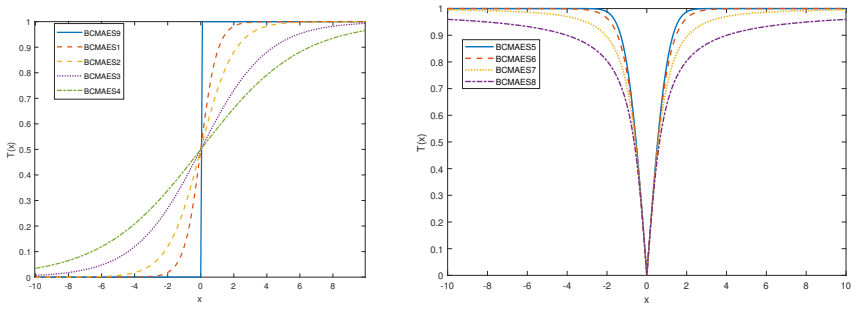

(**a**) BCMAES1- BCMAES4 and BCMAES9. (**b**) BCMAES5- BCMAES8

Figure 3. Symmetric Transfer functions of five BSPSO variants.

BCMAES1–BCMAES9 are shown in Table 1. S1 is steepest, and when x is greater than 4 (or less than -4), the probability value is already close to 1 (or 0). S4 is the smoothest, with a probability of 0.9 when x is 6. The new population of binary variables is generated as:

$$u_{j,t}(k+1) = \begin{cases} 1, & \text{if } \text{rand}_3 < P(v_i(k+1)) \\ 0 & \text{otherwise} \end{cases} \tag{20}$$

BCMAES1–BCMAES9 were used to simulate 10, 20, 60, and 100 fundamental UC problems. The simulation results are shown in Table 4. BCMAES9 was found to have the best effect, so its corresponding transfer function is applied to the following simulation examples.

Table 4. Simulation results for different UC problems using different discretization methods.

	20 units			40 units		
	Min	Avg	Max	Min	Avg	Max
P1	1.123221	1.12388	1.124417	2.243555	2.245358	2.246763
P2	1.123977	1.124316	1.124769	2.245769	2.24592	2.246111
P3	1.123648	1.124027	1.124217	2.245177	2.246111	2.247369
P4	1.123206	1.123886	1.124233	2.245596	2.245699	2.24588
P5	1.126278	1.126411	1.126614	2.263263	2.263433	2.26362
P6	1.12635	1.126357	1.126371	2.262673	2.263645	2.264279
P7	1.126382	1.126395	1.126422	2.264021	2.264067	2.264091
P8	1.126309	1.126694	1.127319	2.265278	2.266509	2.268025
P9	1.123206	1.123933	1.124379	2.243815	2.244699	2.245697
	60 units			100 units		
	Min	Avg	Max	Min	Avg	Max
P1	3.364839	3.365072	3.365532	5.608112	5.612727	5.615718
P2	3.364664	3.365765	3.367682	5.608446	5.610708	5.61394
P3	3.364791	3.365063	3.365276	5.606325	5.610009	5.614433
P4	3.364981	3.365393	3.365878	5.615403	5.61664	5.617814
P5	3.384527	3.384724	3.384929	5.668662	5.669071	5.669827
P6	3.383945	3.384454	3.384881	5.668573	5.669215	5.670004
P7	3.386345	3.386472	3.386562	5.673508	5.674349	5.674773
P8	3.393635	3.395331	3.397049	5.698824	5.705164	5.710726
P9	3.363243	3.364866	3.366701	5.605761	5.611051	5.612635

According to Table 4, in the simulation test of 20 units, BCMAES9 achieved the optimal minimum value of 1.123206 and the maximum value of 1.1243794, while BCMAES1 achieved the best average value of 1.1239328. The minimum and average values of 40 units are 1.123221 for BCMAES1 and 1.234880 for BCMEAS9, respectively. For two large-scale problems of 80 units and 100 units, the best minimum values of 3.363243 and 5.605761 were achieved, respectively. It is clear that BCMAES9 is significantly better than other discretization methods, so we use BCMAES9 as the discretization method used in all subsequent simulation experiments.

3.2.2. The Main Steps of the CMAES Algorithm

The adaptive mechanism of the CMAES algorithm mainly consists of the adaptive covariance and the adaptive global step size. The evolution path and vector difference of the best individuals in the current and previous generations adjusts the covariance matrix.

- Sampling.
  In the CMA evolution strategy, a set of new search points with algebras of $g = 0, 1, 2, \ldots$ are generated by sampling the multivariate normal distribution. The basic formula of sampling is:

$$x_k^{(g+1)} \sim m^{(g)} + \sigma^{(g)} N\left(0, C^{(g)}\right) \quad \text{for} \quad k = 1, \ldots, \lambda \tag{21}$$

$N(0, C^{(g)})$ is a multivariate normal distribution with zero mean and covariance matrix C^g , $x_k^{(g+1)} \in R^n$ is the kth offspring (individual, search point) from the $g+1$ generation, m^g is the average of the gth generation search distribution, and $\sigma^{(g)} \in R_+$ is the overall standard deviation in the gth generation, namely step size;

- Selection and recombination.
  The new mean m^{g+1} is updated by the weighted mean of the sample data $x_1^{(g+1)}, \ldots, x_\lambda^{(g+1)}$:

$$m^{(g+1)} = \sum_{i=1}^{\mu} \omega_i x_{i:\lambda}^{(g+1)} \tag{22}$$

  where

$$\sum_{i=1}^{\mu} \omega_i = 1, \quad \omega_1 \geq \omega_2 \geq \ldots \geq \omega_\mu > 0 \tag{23}$$

  where $\mu \leq \lambda$ is the parent population size and $\omega_{i=1\ldots\mu} \in R_+$ is the weight coefficient of recombination. For $\omega_{i=1\ldots\mu} = 1/\mu$, the formula (29) calculates the average of the selected points, and $x_{i:\lambda}^{(g+1)}$ denotes the optimal ith individual selected from $x_i^{(g+1)}, \ldots, x_\lambda^{(g+1)}$ of (28);
- Update of covariance matrix and step size.
  The update formula of covariance matrix is

$$C^{(g+1)} = \left(1 - c_1 - c_\mu\right) C^{(g)} + c_1 p_c^{(g+1)} \left(p_c^{(g+1)}\right)^T + c_\mu \sum_{i=1}^{\mu} \omega_i y_{i:\lambda}^{(g+1)} \left(y_{i:\lambda}^{(g+1)}\right)^T \tag{24}$$

  where $c_1 \approx 2/n^2$, $c_\mu = \min(\mu_{eff}/n^2, 1 - c_1)$.
  The update formula for the step size is

$$\sigma^{g+1} = \sigma^g + \exp\left(\frac{c_\sigma}{d_\sigma}\left(\frac{\left\|p_\sigma^{g+1}\right\|}{E\|N(0, I)\|}\right)\right) \tag{25}$$

  where $d_\sigma \approx 1$ denotes the damping parameter and $E\|N(0, I)\|$ denotes the expectation of the Euclidean norm of $N(0, I)$ distributed random variables.

3.2.3. Elite Retention Strategy

The GA algorithm originally proposed the elite retention strategy in the application process, and its optimization process is also the process of population evolution. The value of the objective function is defined as the fitness. The higher the fitness, the better the individual performance, closer to the global optimal value. The optimal individual in each generation is defined as the elite individual. The GA algorithm uses selection, crossover, mutation, and other operations for population evolution. However, these updating operations may destroy the optimal individual or increase the time to find the optimal one. Therefore, preserving the optimal individual in the population should be considered.

A similar strategy is adopted here. In the evolution process, considering that updating the parameters will destroy the original optimal individual, the optimal global individual is retained to replace the worst individual in the population, which is the individual with the lowest fitness function. Therefore, the elite retention strategy is divided into two steps, retention followed by replacement, mostly after sampling the original algorithm.

The idea of retaining the global optimal solution mainly comes from the concept of a greedy algorithm. This first considers finding the local optimal solution in the searching process, then gradually approaching the global optimal solution. The formula for retaining elite individuals is given as follows:

$$x_{\text{best}}^{(g)} = \begin{cases} x_k^{(g)}, & \text{if fitness } (k) > gbest^{(g-1)} \\ x_{\text{best}}^{(g-1)}, & \text{otherwise} \end{cases} \tag{26}$$

$$\text{gbest}^{(g)} = \begin{cases} \text{fitness } (k), \text{ if fitness } > \text{ gbest}^{(g-1)} \\ \text{gbest}^{(g-1)}, \text{ otherwise} \end{cases} \tag{27}$$

Here, $x_{best}^{(g)}$ represents the optimal individual of the gth generation and $x_{best}^{(g-1)}$ represents the optimal individual of the previous generation. Similarly, $gbest(g)$ represents the global optimal value of the gth generation and $gbest(g-1)$ is the global optimal value in the population evolving to the previous generation. $fitness(k)$ denotes the fitness function of the kth individual. If the fitness function of an individual is greater than the original global optimal value, the new elite individual replaces the original global optimal individual.

The formula of the substitution operation is as follows:

$$\text{worst } = \min(\text{fitness } (1), \ldots, \text{fitness } (\lambda)) \tag{28}$$

where the worst represents the worst individual value in the population of the generation, the worst individual is found by based on (35).

Among them, *worst* is the value of the worst individual in the population of this generation. The value of the worst individual is found by (40), and thus the $worstIndex$ (the index number of the individual position in the population) of the worst individual is found. Finally, the worst individual in the population can be directly replaced with the optimal individual as follows:

$$x^{(g)}(\text{worstIndex}) = x_{\text{best}}^{(g)} \tag{29}$$

3.2.4. Restart Strategy

The parameter setting heavily impacts the performance of an evolutionary algorithm. This algorithm uses the default parameters provided by Hansen [13]. Selecting a suitable population size has a crucial impact on the performance of an algorithm. To expand the global search ability of the algorithm and improve its convergence speed and computational efficiency, a restart strategy is proposed to adjust it adaptively. The restart strategy implies that the entire algorithm is restarted when the stop criterion is reached, and the population size is increased by n times. The initial population size will still use the default parameters, while the expansion factor is generally selected to be between 1.5 and 5, which is a reasonable choice. The expansion factor determined by the proposed algorithm is chosen to be 2. The flowchart of the BCMAES algorithm is shown in Figure 4.

The stopping criteria of the restart strategy of the algorithm are set as follows according to its properties:

1. If the optimal function value of the last $10 + [30n/\lambda]$ generations is 0 or the absolute difference between the latest function value and the previous function value is less than the given number 10–12;
2. If the standard deviation of the normal distribution is less than in all coordinates and p_σ (the evolutionary path) is less than 10^{-12} in all components;
3. If a standard deviation of 0.1 is added in the direction of the principal axis of $C^{(g)}$, the vector $x_k^{(g)}$ does not change;
4. If a standard deviation of 0.2 is added to each coordinate, $x_k^{(g)}$ does not change;
5. If the condition number of the covariance matrix exceeds 10^{14} .

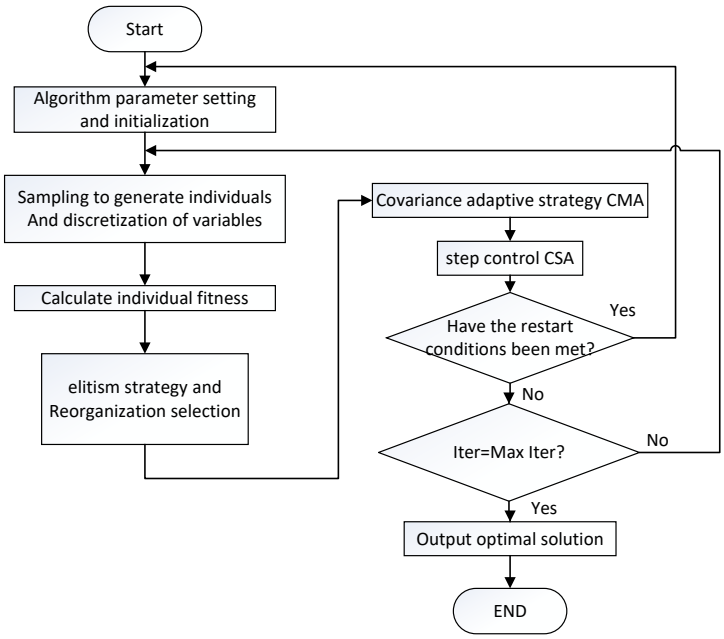

Figure 4. BCMAES algorithm flowchart.

4. Implementation of BCMAES in the UC Problem

When solving the fundamental UC problem, UCEV problem, and UCEVR problem based on BCMAES, because EVs and RE are added to the system, there are some differences in the expression of the solution, the specific implementation of the algorithm, and the corresponding constraint processing methods. This paper will detail the specific implementation steps and constraint processing methods of BCMAES in different models.

4.1. Algorithm Procedure

The algorithm implementation steps of BCMAES in unit commitment problem are given as follows:

Step 1: Initialize the parameters. Initialize the parameters of BCMAES and the parameters of units, electric vehicles, and renewable energy;

Step 2: Population initialization. The initial search point of the BCMAES algorithm is randomly generated, and the electric vehicle's state, output power, and initial output are randomly generated according to the initial variables;

Step 3: Adjust the constraints. Firstly, the initial power of the electric vehicle is adjusted to meet the limitations on the number of electric vehicles, the upper and lower limits of power, and the balance of charge and discharge. Then the minimum start-stop planning and spinning reserve of the whole unit system are adjusted. Through this approach, the start-stop state of the unit can be determined;

Step 4: Economic load schedule. The Lambda iteration method [30] is used to solve the economic scheduling problem while solving the power-balance constraints of the unit and the upper and lower limits of the unit power to determine the output power of each unit.Calculate the maximum power generation of the operating unit. If the system load is less than the entire power generation of the functional unit and the power-balance difference is greater than the set value (0.01 here), Lambda iteration is performed. The process is shown in Figure 5;

Step 5: Calculate the objective function. Calculate the start-up cost and combustion cost of all units in unit time. By comparing the greedy algorithm with the minimum cost of the current iteration each time, if it is less than the minimum cost, it is replaced by a new minimum cost, the optimal function value;

Step 6: update the population through the BCMAES algorithm basic sampling, selection, and reorganization to update the covariance matrix C, update the mean m, and generate new populations and individuals;

Step 7: Termination conditions. Repeat steps 1–6 until the maximum number of iterations is reached.

The steps of solving these problems with BCMAES are similar to those listed above. The flowchart of the BCMAES algorithm for solving the UCEVR problem is illustrated in Figure 6, while the flowcharts for the other two models are quite similar to that shown in Figure 6.

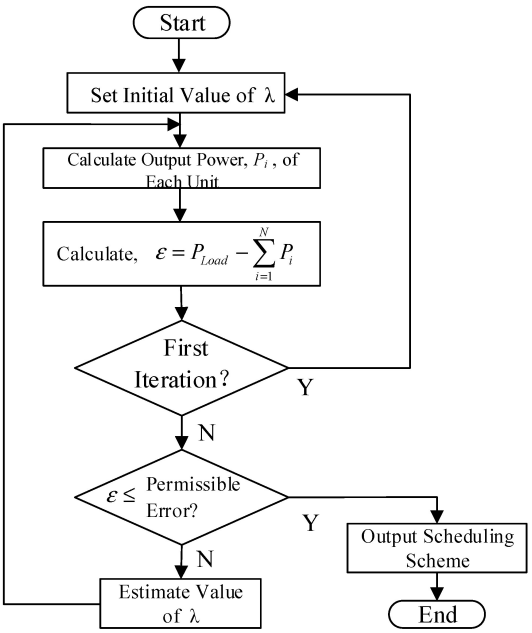

Figure 5. Lambda iterative method to solve the economic scheduling algorithm flow chart.

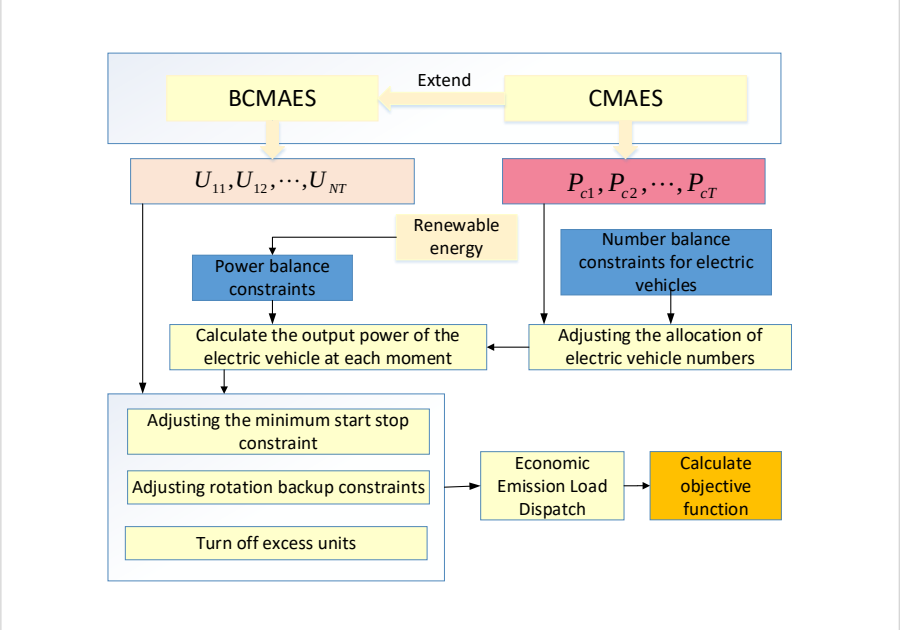

Figure 6. The system framework diagram of the UCEVR problem.

4.2. Encoding of the Solution

When the BCMAES algorithm is used to implement practical applications, all variables are stored in a sample library vector pop as follows:

$$pop = \begin{bmatrix} X_1 & \dots & X_k & \dots & X_{\max} \end{bmatrix} \tag{30}$$

where X_1 is the first variable of the sample library, X_k is the kth vector in the solution vector space (the kth individual in the population), and X_{max} is the last variable in the solution vector space. Although the algorithm has a similar solution structure in different models, the realization of the specific solution is quite different, as shown below:

- Basic UC problem
$$pop = [U_{11}, U_{12}, \dots, U_{1T}, \dots, U_{NT}] \tag{31}$$
- UCEV problem
$$pop = [U_{11}, U_{12}, \dots, U_{1T}, \dots U_{NT}, P_{c1}, \dots, P_{cT}] \tag{32}$$
- UCEVR problem
$$pop = [U_{11}, U_{12}, \dots, U_{1T}, \dots U_{NT}, P_{c1}, \dots, P_{cT}] \tag{33}$$

Although renewable energy (solar and wind) is introduced, it is a fixed constant at each time, so it does not change the structure of the solution of the model. So, it has the same structure as that of the UCEV solution.

4.3. Constraint Processing

4.3.1. Constraint Handling

- Minimum start-stop time constraint of unit
Because the state of each unit at the characteristic time point in a day is affected by the state of the previous time point or even the state of the unit at several time points, they affect each other and couple with each other. Therefore, it is necessary to adjust the unit's start-stop state to meet its minimum start-stop constraint;
- Unit spinning reserve constraint
After the minimum start-stop constraint of the unit is completed, the spinning reserve constraint of the unit should be carried out to ensure safe and stable operation. The core steps of adjusting the spinning reserve constraint can be divided into the following:
- Minimize the number of boot constraints
The system may have redundant startup units when the spinning reserve constraint is adjusted. Therefore, it is necessary to minimize the operation of redundant units and reduce the operation costs of units while maintaining the stable operation of the power system;
- Power-balance constraints
When the above constraints are adjusted, the unit state is also determined. At this time, it is necessary to allocate the unit output power of each period to meet the power-balance constraint, which is the famous economic load dispatch problem. There are many mature and effective ways to solve this problem. The BCMAES algorithm adopts the traditional mathematical method, the Lambda iteration method, to solve this problem, which is convenient and fast.

4.3.2. Constraint Handling in Electric Vehicle Discharge Mode

- Electric vehicle number constraint.
When the BCMAES algorithm is randomly initialized, $N_{EV}(t)$, the balance constraint may not be met. The number of electric vehicles at each moment can be considered a random adjustment process. The number of electric vehicles at one moment is randomly selected. Then the sum of the number of electric vehicles at all moments is

adjusted, and the number difference is calculated. The number of electric vehicles is repeated to meet the number of electric vehicles needed to meet the number constraint of electric vehicles;

- Electric vehicle load power constraints.
  The output power of electric vehicles in the model needs to meet certain restrictions. In particular, in the process of adjusting to meet the number constraints of electric vehicles, this process may generate new electric vehicle output that does not meet the load power constraints of electric vehicles. As with the general boundary treatment method, the endpoint method is used here to obtain the boundary value of the variable that crosses the boundary;
- Power-balance constraint and spinning reserve constraint.
  The V2G mode of electric vehicles is mainly based on the basic UC problem model, which mainly increases the charging of electric vehicles. This violates the original power-balance constraint and spinning reserve constraint. The original power-balance constraint and spinning reserve constraint are changed as follows:

$$\begin{cases} \sum_{i=1}^{N} P_{\mathrm{u},i}(t)U_i(t) = Pd(t) \\ \sum_{i=1}^{N} P_{u,i}^{\max} >= Pd(t) \times (1+SR) \end{cases} \rightarrow \begin{cases} \sum_{i=1}^{N} P_{\mathrm{u},i}(t)U_i(t) + P_c(t) = Pd(t) \\ \sum_{i=1}^{N} P_{u,i}^{\max} + P_{c,\max}(t) >= Pd(t) \times (1+SR) \end{cases} \tag{34}$$

4.3.3. Constraint Handling in Charging and Discharging Mode of the Electric Vehicle

The UCEV (V2G/G2V) problem is mainly based on the UCEV (V2G) model, which adds a charge-discharge balance constraint on all the original conditions. In the UCEV (V2G) model, the electric vehicle is discharging at every moment, but the UCEV (V2G/G2V) model considers another mode, that is, charging at some point in the day, discharging at some point, and ensuring that the amounts of charge and discharge during the day are equal.

4.3.4. Renewable Energy Constraint Handling

Under the premise of electric vehicles connected to the grid, renewable energy is incorporated, mainly increasing amounts of wind and solar energy. In this situation, the original power-balance constraint and spinning reserve constraint are violated.

$$\begin{cases} \sum_{i=1}^{N} P_{\mathrm{u},i}(t)U_i(t) + P_w(t) + P_s(t) + P_c(t) = Pd(t) \\ \sum_{i=1}^{N} P_{u,i}^{\max} + \eta_R(P_{\mathrm{w}}(t) + P_s(t)) + P_{c,\max}(t) >= Pd(t) \times (1+SR) \end{cases} \tag{35}$$

From the above formula, it is easy to see that, although in the original formula, the increase in the output power of renewable energy invalidates the original formula. In the UCEVR model, the wind power output power $P_w(t)$, solar power output power $P_s(t)$, and η_R are constants, so there is no destructive change to the whole constraint, only the original constraint condition needs to be modified.

5. Analysis of Simulation Results

The algorithm program runs in the Matlab 2019b environment of a desktop PC with an Intel (R) Core (TM) i7-8700 K CPU 3.70 GHz, 32 GB memory, and Windows 10 operating system. This paper uses the proposed BCMAES algorithm to solve different UC models. Several different simulation experiments are designed for comparison and analysis to verify the algorithm's effectiveness. This chapter deals mainly with the simulating of the basic UC model. The initialization parameters of the algorithm are shown in the study by Hansen [13].

5.1. Ten Fundamental UC Problems

This section uses the BCMAES algorithm to simulate the basic UC model and compare this simulations by other algorithms. Yang et al., 2023 [31] gives the system load of the IEEE-10 standard unit commitment problem. The spinning reserve of unexpected generator outages and prediction errors is 10% of the hourly demand load (SR = 10%). The study shows each unit's characteristic parameters, initial state information, start-up cost, and minimum switching time. All parameters are obtained from Hansen [13].

The parameter values of each algorithm remain unchanged, and the same constraint processing method is adopted. Thirty independent simulation experiments are carried out on the unit commitment example. Each experiment's maximum function evaluation (FES) is 50,000.

We can apply our proposed BCMAES algorithm to the basic UC model based on the above data. To better verify the performance of the algorithm, we compare the results obtained by the BCMAES algorithm with some excellent algorithms in the literature for the same model. The results are shown in Table 5.

Table 5. Cost comparison of different algorithms.

	Minimum Cost (USD)	Average Cost (USD)	Maximum Cost (USD)	Standard Deviation
GA	565,825	-	570,032	-
EP	564,554	-	566,231	-
SA	565,828	565,988	566,260	-
BCGA	567,367	-	-	-
FPGA	564,094	566,675	569,237	-
ICGA	566,404	-	-	-
MRCGA	564,244	564,467	565,756	-
LR	565,825	-	-	-
PSOLR	565,869	-	566,793	-
QEA	563,938	564,672	563,969	-
IQEA	563,977	563,977	563,977	0
IPSO	563,954	564,162	564,579	-
IBPSO	563,977	564,155	565,312	143
QBPSO	563,977	563,977	563,977	0
ATHS	563,938	-	-	-
HHS	563,937	563,965	563,995	-
NBPSO	563,937	563,962	563,977	-
BCSO	563,937	563,937	563,937	0
HS	568,685	569,029	569,296	175
TLBO	566,779	567,017	567,173	258
BPSO	563,975	564,129	564,618	274
BCMAES	563,937	563,937	563,937	0

Table 6 shows the unit state and output required by BCMAES to achieve the minimum cost per hour on 10 basic UC problems and lists the related operating costs per hour. It can also be seen that more units are opened during the peak period of corresponding load demand, and high-power units with low-cost coefficients are preferentially opened.

5.2. Basic UC Problem of High-Dimensional Unit

To verify the effect of the BCMAES algorithm in high-dimensional units, the original standard example is extended. The simulation experiments are carried out on 20, 40, 60, 80, and 100 units, respectively. The system's load is expanded to 2, 4, 6, 8, and 10 times the original, and the parameters of other units remain unchanged. Due to the expansion of the scale of the problem, the FES of the example is also expanded to the unit expansion multiple of the original FES, and 30 simulation experiments are still carried out independently. The comparison results of the BCMAES algorithm with other algorithms in high-dimensional units are shown in Table 7.

Table 6. Optimal solutions by BCMAES for UC with 10 units.

Time	Unit Output										Start-Up Cost/USD
	1	2	3	4	5	6	7	8	9	10	
1	455	245	0	0	0	0	0	0	0	0	0
2	455	295	0	0	0	0	0	0	0	0	0
3	455	370	0	0	25	0	0	0	0	0	900
4	455	455	0	0	40	0	0	0	0	0	0
5	455	390	0	130	25	0	0	0	0	0	560
6	455	360	130	130	25	0	0	0	0	0	1100
7	455	410	130	130	25	0	0	0	0	0	0
8	455	455	130	130	30	0	0	0	0	0	0
9	455	455	130	130	85	20	25	0	0	0	860
10	455	455	130	130	162	33	25	10	0	0	60
11	455	455	130	130	162	73	25	10	0	0	60
12	455	455	130	130	162	80	25	43	10	10	60
13	455	455	130	130	162	33	25	10	0	0	0
14	455	455	130	130	85	20	25	0	0	0	0
15	455	455	130	130	30	0	0	0	0	0	0
16	455	310	130	130	25	0	0	0	0	0	0
17	455	260	130	130	25	0	0	0	0	0	0
18	455	360	130	130	25	0	0	0	0	0	0
19	455	455	130	130	30	0	0	0	0	0	0
20	455	455	130	130	162	33	25	10	0	0	490
21	455	455	130	130	85	20	25	0	0	0	0
22	455	455	0	0	145	20	25	0	0	0	0
23	455	420	0	0	0	20	0	0	0	0	0
24	455	345	0	0	0	0	0	0	0	0	0
Total cost: USD 563,937											

It can be seen from Table 7 that many algorithms may have better performance in low-dimensional units. However, when the number of dimensions is expanded, algorithmic performance is greatly affected by the size, and many algorithms on high-dimensional units are entirely uncompetitive. Furthermore, the simulation experiment in the high-dimensional unit can enlarge the difference in performance between the algorithms, allowing the difference in the performance of each algorithm to be more easily compared. The above table shows that the BCMAES algorithm performs slightly worse than the QEA algorithm on 20 units but can still obtain the optimal solution compared with other algorithms on high-dimensional units. Therefore, it can be concluded that the BCMAES algorithm is an excellent algorithm for solving binary problems and is not affected by the dimension of the problem. Furthermore, with the expansion of the scale of the problem, the differences between different algorithms are becoming increasingly obvious. Figure 7 shows the convergence curves of the HS, TLBO, BPSO, and BCMAES algorithms in high-dimensional units.

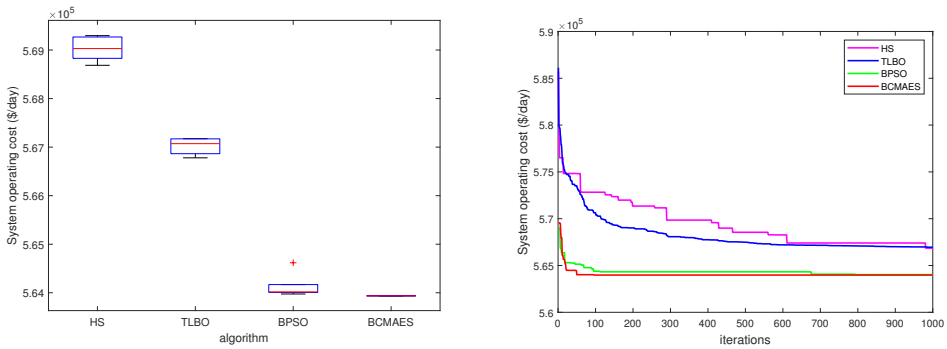

(**a**) Comparison of simulation results. (**b**) Comparison of convergence curves.

Figure 7. Comparison of four different algorithms.

It can be seen from Figure 7 that with the expansion of the unit dimension, the performance differences between each algorithm are getting larger and larger. When there are 100 units, the BCMAES algorithm is far superior to the other three algorithms in the quality of the solution. As the scale of the unit continues to expand, the convergence of all algorithms worsens. Even though BCAMES solves high-dimensional units, the convergence of the algorithm is worse than that of low-dimensional units. The convergence speed of BCMAES is always less than HS and TLBO, and sometimes less than BPSO. BPSO quickly converges prematurely and produces poor solutions.

5.3. IEEE 118-Bus System with 54 Units Problems

The IEEE 118-bus system with 54 thermal generation units is used in this case study. The system configuration data is given in [32], while the load data for 24 h duration along with reserves are given in [33]. Fuel cost functions of all the units are assumed to be quadratic in nature. The ramp rate constraint is also taken into account along with the spinning reserve constraint. Transmission losses are neglected in this case. Under these conditions, the best cost value obtained in 30 trial runs is USD 1,624,873.6, which is less than the USD 1,636,381.0 that is achieved using ABSSA [34] and the USD 1,643,750.0 that is obtained using B&B-IPM [35]. The unit commitment status for the 54 thermal units is given in [31]. A comparison of the cost over 30 runs of a 54-unit system is given in Table 8.

Table 7. Performance comparison of BCMAES with other algorithm for UC with high dimensions.

Type	Minimum Operating Costs (USD)				
	20 Units	**40 Units**	**60 Units**	**80 Units**	**100 Units**
GA	1,126,243	2,251,911	3,376,625	4,504,933	5,627,437
EP	1,127,257	2,252,612	3,376,255	4,505,536	5,633,800
SA [28]	1,126,251	2,250,063	–	4,498,076	5,617,876
BCGA	1,130,291	2,256,590	3,382,913	4,511,438	5,637,930
FPGA [36]	1,124,998	2,248,235	3,368,375	4,491,169	5,614,357
ICGA	1,127,244	2,254,123	3,378,108	4,498,943	5,630,838
MRCGA [37]	1,127,244	2,254,123	3,378,108	4,498,943	5,630,838
LR	1,130,660	2,258,503	3,394,066	4,526,022	5,657,277
PSOLR	1,128,072	2,251,116	3,376,407	4,496,717	5,623,607
QEA [38]	1,123,607	2,245,557	3,366,676	4,488,470	5,609,550
IPSO [39]	1,125,279	2,248,163	3,370,979	4,495,032	5,619,284
IBPSO [38]	1,125,276	2,248,581	3,367,865	4,491,083	5,610,293
HS	1,132,029	2,271,188	3,410,737	4,553,929	5,697,561
TLBO	1,131,247	2,286,549	3,425,802	4,587,544	5,747,395
BPSO	1,130,597	2,271,170	3,413,645	4,579,435	5,717,184
BGOA [40]	1,120,470	2,240,277	3,356,574	4,475,407	5,596,414
ABFMO [41]	1,131,551	2,265,867	3,397,162	4,531,605	5,660,087
LS-MFA [31]	1,123,297	2,240,277	3,363,491	4,475,407	5,604,146
BSLPSO [26]	1,124,389	2,246,837	3,367,349	4,491,179	5,611,494
BCMAES	1,124,202	2,246,621	3,365,137	4,487,337	5,607,082

Table 8. Comparison of cost over 30 runs of a 54-unit system.

Methods	**Total Costs/USD**	**FES**
BB-IPM [35]	1,643,750.0	40,000
PSO [42]	1,635,395.3	40,000
GWO [42]	1,643,852.1	40,000
HGWO-PSO [42]	1,619,385.9	40,000
ABSSA [34]	1,636,381.0	40,000
SDP	1,645,445.0	40,000
ABC-LR	1,644,269.7	40,000
BRCFF	1,644,141.0	40,000
GA [43]	1,644,336.8	40,000
ACS [43]	1,643,968.3	40,000
HTACS [43]	1,643,840.4	40,000
BCMAES	1,624,873.60	40,000

5.4. Unit Commitment Problem with Electric Vehicle Discharge (V2G)

5.4.1. Unit Commitment Problem with Electric Vehicle Discharge (V2G) without Considering Emissions

Various simulation experiments are designed to analyze the influence of electric vehicle grid connection on power systems under different modes. This section mainly describes the simulation comparison under UCEV (V2G) mode. The UCEV problem model comprises grid-connected electric vehicles (all in discharge state within 24 h) and the previous 10 IEEE-10 standard unit systems. The data on electric vehicles can be obtained from the literature. The specific parameters are as Table 9.

Suppose the total number of electric vehicles in a region is 50,000. In that case, the average battery capacity of electric vehicles is 0.015, the average percentage of batteries that electric vehicles need to charge is 50%, and the total efficiency of electric vehicles is 8%. The average output power of the electric vehicle is 0.015 × 50% × 80%. Table 10 shows the minimum number of discharges per hour of electric vehicles in this model.

Table 9. EV parameter settings.

Name	Value
The average battery capacity of electric vehicles, av PV (MW)	0.015
The maximum battery capacity of an electric vehicle, max PV (MW)	0.025
The minimum battery capacity of an electric vehicle, min PV (MW)	0.01
The average percentage of batteries that need to be charged for electric vehicles	50%
Total efficiency, EV	85%

Table 10. Minimal discharge number of EVs per hour.

Hour	N min (*t*)	Hour	N min (*t*)	Hour	N min (*t*)	Hour	N min (*t*)
1	0	7	0	13	3400	19	0
2	0	8	0	14	1500	20	0
3	2000	9	1500	15	0	21	0
4	0	10	3400	16	0	22	0
5	2200	11	3400	17	0	23	0
6	0	12	3400	18	0	24	0

In summary, the BCMAES algorithm is the best choice among these algorithms to solve this UCEV (V2G) problem. At the same time, we can see that after all the algorithms are incorporated into the power grid, the system's minimum, maximum, and average operating costs are reduced to a certain extent. Therefore, integrating electric vehicles can significantly reduce the unit's operational costs and bring significant economic benefits.

Figure 8a compares the hourly running cost of the solution obtained by the BCMAES algorithm on the UCEV problem with the results on the UC problem, and Figure 8b shows the hourly cost savings. It can be seen from Figure 8 that the grid connection of electric vehicles at most moments can save operating costs for the system. The grid connection of electric vehicles at a small number of moments will increase the system's operating costs. Still, those increased costs are generally far less than the reduction in costs, which can be compensated by other periods. In addition, the larger areas of cost savings after adding electric vehicles are concentrated in the peak period.

5.4.2. Unit Commitment Problem with Electric Vehicle Discharge (V2G) Also Considering Emissions

This paper also considers the emission of the 10 units under study. The emission coefficient c and the weight factor e are taken from the literature [4]. When considering emissions in the objective function, the simulation results on the UCEV (V2G) problem using BCMAES and the other algorithms are as shown in Table 11.

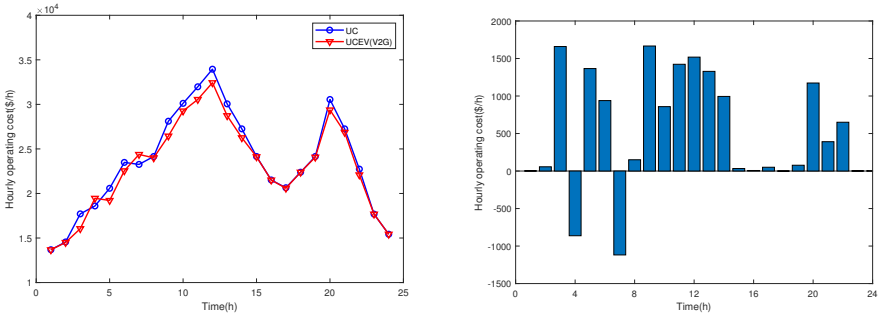

(**a**) Comparison of Results. (**b**) Cost savings per hour.

Figure 8. Comparison of the hourly cost of UCEV (V2G) and UC using BCMAES.

It can be seen from Table 11 that if emissions are considered in a system, some economic benefits will inevitably be sacrificed for sustainable development. The operating cost of the same algorithm in the model with consideration of emissions is less than that in the model without considering emissions. Compared with the model without considering emissions, the optimal cost obtained by the BCMAES algorithm increases by USD 29,551/day, or about 5%.

Table 11. Comparison of BCMAES results with and without considering emissions on UCEV (V2G).

Algorithms	Without Emissions			With Emissions		
	Function	Cost (USD)	Emissions (t)	Function	Cost (USD)	Emissions (t)
PSO [42]	554,509	554,509	-	825,392	565,326	260,066
GA-LR [9]	552,427	552,427	-	-	-	-
GA	556,420	556,420	-	798,183	561,196	236,987
LR	558,389	558,389	-	812,392	559,822	252,570
BCMAES	551,784	551,784	-	760,670	581,335	179,335

Table 12 shows the results of the BCMAES algorithm and other algorithms on the UCEV (V2G) model without considering emissions compared with the results of the model in the previous section to compare and analyze the impact of electric vehicle grid connection on the entire system.

Table 12. Comparison of the results of BCMAES on UCEV (V2G) problem and UC problem.

Algorithms	Basic UC			V2G		
	Minimum	Mean	Maximum	Minimum	Mean	Maximum
PSO [42]	564,714	554,743	565,443	554,509	557,584	559,987
GA-LR [9]	564,703	-	-	552,427	552,965	553,765
GA	565,825	-	570,032	556,420	558,635	560,720
LR	565,825	-	-	558,339	560,034	562,572
BCMAES	563,937	563,937	563,937	551,784	552,277	552,745

5.5. Unit Commitment Problem with Electric Vehicle Charging and Discharging (V2G/G2V)

The main consideration in the previous section is the continuous discharge of electric vehicles within 24 h, but this situation is an ideal model, not close to reality. This section mainly considers both electric vehicle charging and electric vehicle discharging. As shown in Figure 9, the 24 h of the day can be divided into three parts and five periods, including the Valley stage (0:00–5:00), Off-Peak stage (5:00–9:00, 15:00–19:00), and Peak stage (9:00–15:00, 19:00–24:00). Among them, electric vehicles are charged during the Valley phase, and the Off-Peak phase during the two low peaks, and electric vehicles are discharged during the Peak phase during the peak period. Therefore, the probability ratio of charging and discharging electric vehicles in one day is 1:1.

5.5.1. Unit Commitment Problem with Electric Vehicle Charging and Discharging (V2G/G2V) without Considering Emissions

Table 13 compares each algorithm's lowest, average, and maximum optimization cost for 10 UCEV (V2G/G2V) problems. It is evident that BCMAES can also obtain the minimum unit operating cost of USD 558,790/day for more complex constraints. Compared to the other algorithms, it has better optimization ability and stability. When considering the discharge of the EV grid, the total minimum cost increased from USD 551,784/Day to USD 558,790/Day, or about 1.3%. Although the economic cost increases compared to the first model, the second model is closer to the actual situation.

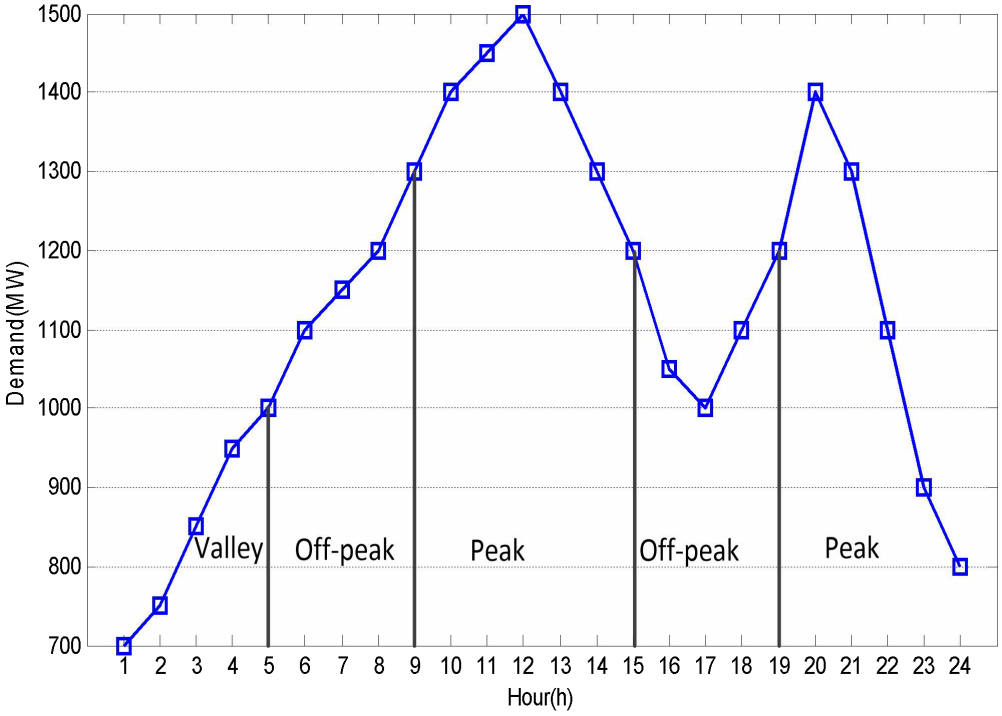

Figure 9. The high and low peak charge and discharge intervals on the load curve.

Table 13. The comparison of the results of different algorithms on solving the UCEV problem in different modes.

Algorithms	V2G			V2G/G2V		
	Minimum	Mean	Maximum	Minimum	Mean	Maximum
PSO [42]	554,509	557,584	559,987	-	-	-
GA-LR [9]	552,427	552,965	553,765	561,821	564,049	566,281
GA	556,420	558,635	560,720	562,301	565,577	568,804
LR	558,339	560,034	562,572	564,795	567,020	568,138
BCMAES	551,784	552,277	552,745	558,790	559,190	559,845

The addition of electric vehicles to the grid brings difficulties to the start-stop and output scheduling of the unit while charging and discharging, but this is closer to the actual situation.

Compared with the situation that electric vehicles are only used as portable energy storage devices, the operating cost of the unit will inevitably increase. Reasonable allocation through optimization algorithms can not only balance the number of charging and discharging events of electric vehicles at all times but also reduce the number of start-stops of the unit, optimize the output power, and significantly reduce costs.

After the charging and discharging of electric vehicles are connected to the grid, because the charging of electric vehicles increases the load demand of the system and the output of the unit, the operating cost of the unit with only discharge will be increased.

However, compared with the basic unit commitment problem, the daily cost savings can reach USD 5147/day, and the economic benefits obtained over time are considerable.

5.5.2. Unit Commitment Problem with Electric Vehicle Charging and Discharging (V2G/G2V) Considering Emissions

When considering emissions in the objective function, the simulation results of BCMAES and the other algorithms on the UCEV problem are given in Table 14.

It can be seen from Table 14 that if emissions are considered in a system, some economic benefits will inevitably be sacrificed for sustainable development. The operating costs of the same algorithm in the model with emissions is greater than that of the model without emissions. For example, the BCMAES algorithm increases the operating costs by USD 26,354/day when considering emissions. The BCMAES algorithm is capable of demonstrating the best optimization ability and robustness in the above comparison. Separately, the algorithm not only has lower operating costs than the other algorithms but also has lower emissions than the other algorithms. Therefore, the use of the BCMAES algorithm can not only bring good economic effects but also reduce emissions for sustainable development.

Table 14. Comparison of BCMAES results with and without considering emissions for UCEV (V2G/G2V).

Algorithms	without Emission			Emission		
	Function	Cost (USD)	Emission (t)	Function	Cost (USD)	Emission (t)
PSO [42]	-	-	-	-	-	-
GA-LR [9]	561,821	561,821	-	-	-	-
GA	563,361	563,361	-	806,485	566,939	239,546
LR	564,795	564,795	-	801,484	570,265	231,219
BCMAES	558,790	558,790	-	769,187	585,144	184,043

Table 15 shows the comparison of the results of different algorithms in solving the UCEV problem in different modes when considering emissions. Not only the GA algorithm but also the other two algorithms in the V2G/G2V mode have increased in cost, but the emissions have been reduced considerably, and the overall objective function has also been reduced. This shows that the V2G/G2V mode of electric vehicle grid connection can better maintain the balance between cost and emission than the V2G mode and better adapt to the needs of the sustainable development of power systems in modern society. The optimal solution obtained by the BCMAES algorithm is in the V2G/G2V mode not the V2G mode. However, the operating cost is reduced by about 0.77%, and emissions are increased by about 8.49%, so the final objective function is also increased by about 1.3%. Still, this model is closer to the actual production and operational conditions.

Table 15. Comparison of the results of UCEV in different modes when considering emissions.

Algorithms	without Emission			Emission		
	Function	Cost (USD)	Emission (t)	Function	Cost (USD)	Emission (t)
PSO [42]	825,392	565,326	260,066	-	-	-
GA-LR [9]	-	-	-	-	-	-
GA	798,183	561,196	236,987	806,485	566,939	239,546
LR	812,392	559,822	252,570	801,484	570,265	231,219
BCMAES	759,346	589,709	169,637	769,187	585,144	184,043

5.6. Unit Commitment Problem with Electric Vehicles and Renewable Energy

In this section, the UCEVR problem considers 10 wind energy and solar energy production scenarios. In this model, emissions are considered, and different EV grid-connected operation modes are considered. Therefore, the latter comparison is based on the UCEV problem considering emissions. Table 16 shows the optimal unit economic

cost and performance indicators using the BCMAES algorithm in 10 wind power scenarios. It can be seen that the values of different performance indicators change very little. In the case of the highest Sec, we will select Wind Scenario 5, use it in the following studies, and mark it in bold.

After integrating renewable energy into the grid, the daily power generation cost is USD 552,578 and daily emissions are 158,816 tons, reductions of nearly 5.57% and 13.71%, respectively. This represents an annual saving of USD 11,886,590 in production costs and an annual reduction of 9,207,855 tons in emissions.

Figure 10 shows the number of electric vehicles in a 10-unit system with or without renewable energy within 24 h. V2G electric vehicles are expressed as positive, while G2V electric vehicles are described as negative. As shown in Figure 10a, when only V2G EVs are connected to the grid, intermittent wind power has two significant differences, between 1:00–6:00 in the morning and between 14:00 and 24:00 in the evening. In Figure 10b, the apparent changes in electric vehicles occur at 5:00 to 8:00 in the morning, 9:00 to 12:00 in the morning, 15:00 to 17:00 in the afternoon, and 20:00 to 24:00 in the evening.

Table 16. The optimal unit economic cost and performance index of 10 wind energy scenarios.

Model	Scene	Cost	Emission	Index 1	Index 2	Sce
discharge	1	543,942	150,849	0.09996	0.09902	0.6181
	2	542,971	150,901	0.09983	0.10015	0.445
	3	540,552	154,201	0.09996	0.1017	0.357
	4	542,525	151,427	0.09984	0.09824	0.2802
	5	542,633	153,297	0.10012	0.09932	0.8298
	6	545,941	150,218	0.10016	0.09967	0.3828
	7	540,347	154,295	0.09994	0.10088	0.7021
	8	541,260	153,444	0.09995	0.10087	0.6449
	9	544,800	151,161	0.10013	0.10038	0.4638
	10	540,427	155,466	0.10012	0.09972	0.2752
charge	1	548,044	165,029	0.1002	0.09902	0.6174
	2	550,253	162,764	0.10019	0.10015	0.4442
	3	550,035	162,083	0.10007	0.1017	0.3568
	4	553,040	159,041	0.10006	0.09824	0.2824
	5	552,578	158,816	0.09997	0.09932	0.8326
	6	551,092	159,438	0.09984	0.09967	0.3859
	7	554,306	156,440	0.09988	0.10088	0.7023
	8	552,564	159,050	0.10000	0.10087	0.6472
	9	553,382	157,813	0.09993	0.10038	0.4642
	10	551,809	158,732	0.09984	0.09972	0.2806

Figure 11 describes the power requirements of each unit across 24 h. In Figure 11a, the blue bars indicates the power demand in each hour of the 24 h. As V2G electric vehicles provide power to meet local load demand, the unit demand for thermal units will decrease, as shown by the red bars. When the RE is connected to the grid, the power demand of the thermal units shown by the green bars will be further reduced. Figure 11b shows the unit's power output under V2G/G2V. It can be seen that the cooling unit needs to generate more power during the charging of G2V electric vehicles. However, RE can compensate for the additional load demand caused by G2V electric vehicles. Therefore, the cooperation between electric vehicles and renewable energy can reduce the load demand pressure of the system, especially the additional charging demand brought by G2V electric vehicles.

Figure 12 shows the spinning reserve of the system of 10 units across 24 h. In Figure 12a, although the number of devices is reduced when renewable energy is connected to the grid, in the case of UCEVR (V2G), the spinning reserve is more rugged than in the case of UCEV (V2G). As shown in Figure 12b, for most of the 24 h, the spinning reserve with renewable energy is rather higher than that without considering renewable energy during the charging period. Therefore, integrating electric vehicles and renewable energy into the power system can reduce the spinning reserve's violent fluctuations and improve the UCEVR system's reliability.

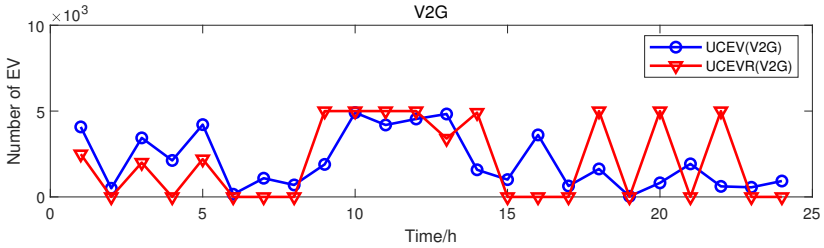

(**a**) The power output of the cell under V2G.

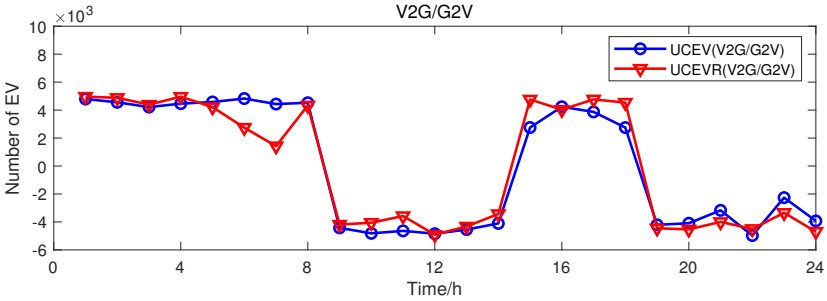

(**b**) The power output of the cell under V2G / G2V.

Figure 10. The number of electric vehicles incorporated into the grid in a 24-h period.

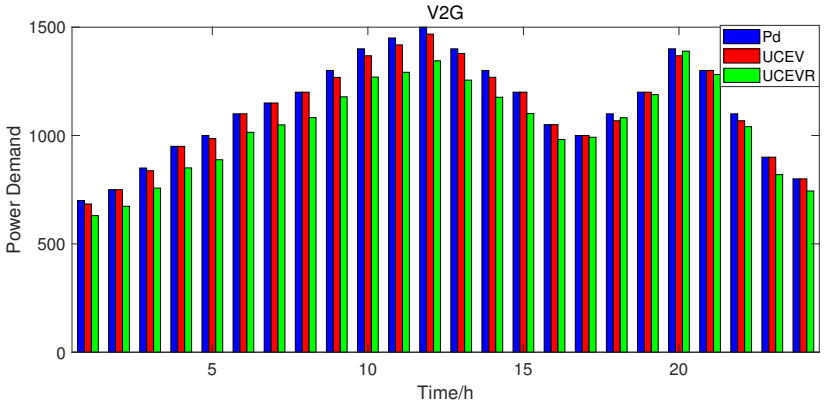

(**a**) V2G.

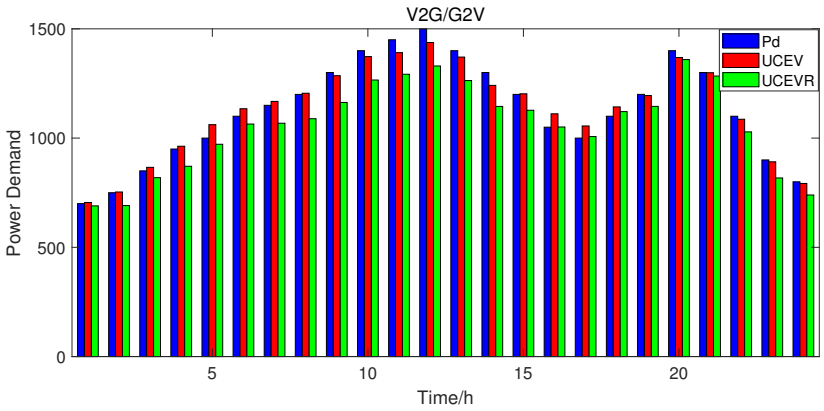

(**b**) V2G/G2V.

Figure 11. The power demand of the unit across 24 h.

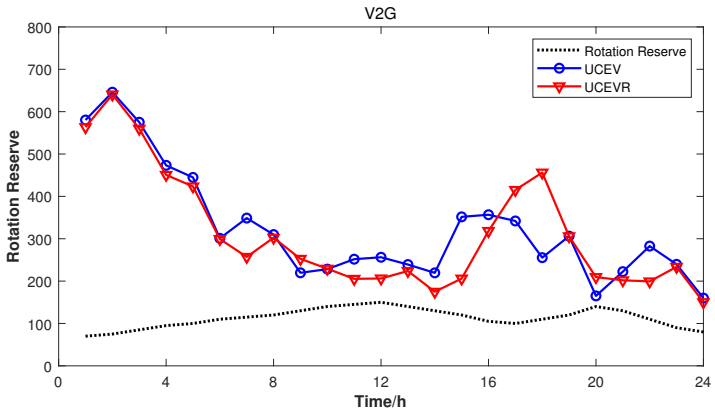

(**a**) Spinning reserve across 24 h under V2G.

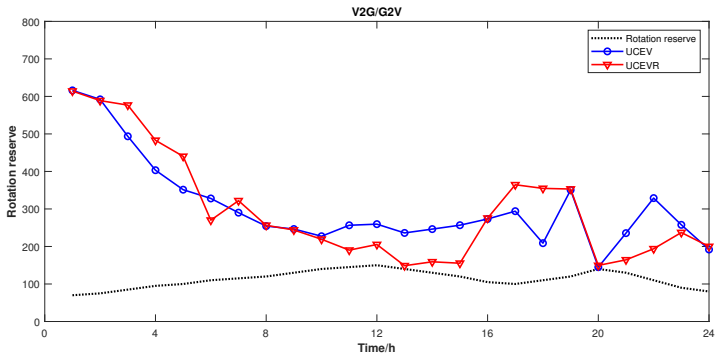

(**b**) Spinning reserve across 24 h under V2G/G2V.

Figure 12. Spinning reserve energy storage across 24 h.

6. Conclusions

This paper has proposed a new binary CMAES algorithm, dubbed BCMAES, to solve complex UC problems for power systems integrated with renewable generations and electric vehicles. To verify the efficacy and effectiveness of the proposed BCMAES algorithm, a comparative study was conducted with several other popular approaches. The simulated experimental tests on power systems of two different scales, 10 and 54 units, show that for the 54-unit system, the proposed algorithm successfully achieved operation costs reduction of USD 1,624,873.6 per day, which is 1.15% more than the other tested methods. The results for the 10-unit power system are also quite similar. The main contributions of this paper are summarized below.

- The CMAES algorithm has been extended to the binary domain by introducing the signal function to map the variables;
- The elite and restart strategies have been introduced to strengthen the algorithm's global search capability and realize its population adaptation;
- The proposed BCMAES algorithm has been tested on power systems with 10 and 54 units and the simulation results confirm its efficacy and robustness in comparison with several popular UC approaches, achieving more than a 1% operation cost reduction in most cases;
- With the proposed algorithm, the influence of renewable energy integration and EV grid connection modes on the whole system UC is analyzed. It is found that V2G and integration of renewable energy can significantly reduce both the operation costs and emissions by 5.57% and 13.71%, respectively.

Finally, the renewable energy is treated as a deterministic variable in this paper. To assess the impact of stochastic renewable power generations on the UC model will be our future work.

Author Contributions: Q.N. conceptualized and designed experiments; Q.N., Z.Y., L.T. and L.Y. conducted experiments; Q.N. and L.T. analyzed the data; Q.N., H.W. and L.T. wrote and revised the paper. All authors have read and agreed to the published version of the manuscript.

Funding: The research of this article is funded by the National Natural Science Foundation of China [No. 61773252 and 52077213].

Institutional Review Board Statement: Not applicable.

Informed Consent Statement: Not applicable.

Data Availability Statement: Data is contained within the article.

Conflicts of Interest: The authors declare no conflict of interests.

References

1. Ziyaei, S.; Panahi, M.; Manzour, D.; Karbasi, A.; Ghaffarzadeh, H. Sustainable Power Generation through Decarbonization in the Power Generation Industry. *Environ. Monit. Assess.* **2023**, *195*, 225. [CrossRef] [PubMed]
2. Quan, H.; Srinivasan, D.; Khosravi, A. Integration of Renewable Generation Uncertainties into Stochastic Unit Commitment Considering Reserve and Risk: A Comparative Study. *Energy* **2016**, *103*, 735–745. [CrossRef]
3. Bertsimas, D.; Litvinov, E.; Sun, X.A.; Zhao, J.; Zheng, T. Adaptive Robust Optimization for the Security Constrained Unit Commitment Problem. *IEEE Trans. Power Syst.* **2013**, *28*, 52–63. [CrossRef]
4. Saber, A.Y.; Venayagamoorthy, G.K. Intelligent Unit Commitment with Vehicle-to-Grid —A Cost-Emission Optimization. *J. Power Sources* **2010**, *195*, 898–911. [CrossRef]
5. Madzharov, D.; Delarue, E.; D'haeseleer, W. Integrating Electric Vehicles as Flexible Load in Unit Commitment Modeling. *Energy* **2014**, *65*, 285–294. [CrossRef]
6. Talebizadeh, E.; Rashidinejad, M.; Abdollahi, A. Evaluation of Plug-in Electric Vehicles Impact on Cost-Based Unit Commitment. *J. Power Sources* **2014**, *248*, 545–552. [CrossRef]
7. Chen, S.X.; Gooi, H.B.; Wang, M.Q. Sizing of Energy Storage for Microgrids. *IEEE Trans. Smart Grid* **2012**, *3*, 142–151. [CrossRef]
8. Saber, A.Y.; Venayagamoorthy, G.K. Efficient Utilization of Renewable Energy Sources by Gridable Vehicles in Cyber-Physical Energy Systems. *IEEE Syst. J.* **2010**, *4*, 285–294. [CrossRef]
9. Jiang, Q.; Zhou, B.; Zhang, M. Parallel Augment Lagrangian Relaxation Method for Transient Stability Constrained Unit Commitment. *IEEE Trans. Power Syst.* **2013**, *28*, 1140–1148. [CrossRef]
10. Geem, Z.W.; Kim, J.H.; Loganathan, G. A New Heuristic Optimization Algorithm: Harmony Search. *Simulation* **2001**, *76*, 60–68. [CrossRef]
11. Rao, R.; Savsani, V.; Vakharia, D. Teaching–Learning-Based Optimization: A Novel Method for Constrained Mechanical Design Optimization Problems. *Comput. Aided Des.* **2011**, *43*, 303–315. [CrossRef]
12. Han, K.-H.; Jong-Hwan Kim, J.H. Quantum-Inspired Evolutionary Algorithm for a Class of Combinatorial Optimization. *IEEE Trans. Evol. Comput.* **2002**, *6*, 580–593. [CrossRef]
13. Hansen, N. The CMA Evolution Strategy: A Comparing Review. In *Towards a New Evolutionary Computation: Advances in the Estimation of Distribution Algorithms*; Lozano, J.A., Larrañaga, P., Inza, I., Bengoetxea, E., Eds.; Studies in Fuzziness and Soft Computing; Springer: Berlin/Heidelberg, Germany, 2006; pp. 75–102. [CrossRef]
14. Hu, J.; Chen, H.; Heidari, A.A.; Wang, M.; Zhang, X.; Chen, Y.; Pan, Z. Orthogonal Learning Covariance Matrix for Defects of Grey Wolf Optimizer: Insights, Balance, Diversity, and Feature Selection. *Knowl. Based Syst.* **2021**, *213*, 106684. [CrossRef]
15. Li, X.; Yao, X. Cooperatively Coevolving Particle Swarms for Large Scale Optimization. *IEEE Trans. Evol. Comput.* **2012**, *16*, 210–224. [CrossRef]
16. Manoharan, P.S.; Kannan, P.S.; Baskar, S.; Willjuice Iruthayarajan, M.; Dhananjeyan, V. Covariance Matrix Adapted Evolution Strategy Algorithm-Based Solution to Dynamic Economic Dispatch Problems. *Eng. Optim.* **2009**, *41*, 635–657. [CrossRef]
17. Salman, D.; Kusaf, M. Short-Term Unit Commitment by Using Machine Learning to Cover the Uncertainty of Wind Power Forecasting. *Sustainability* **2021**, *13*, 13609. [CrossRef]
18. Jia, Y.H.; Zhou, Y.R.; Lin, Y.; Yu, W.J.; Gao, Y.; Lu, L. A Distributed Cooperative Co-Evolutionary CMA Evolution Strategy for Global Optimization of Large-Scale Overlapping Problems. *IEEE Access* **2019**, *7*, 19821–19834. [CrossRef]
19. Rezk, H.; Olabi, A.G.; Sayed, E.T.; Wilberforce, T. Role of Metaheuristics in Optimizing Microgrids Operating and Management Issues: A Comprehensive Review. *Sustainability* **2023**, *15*, 4982. [CrossRef]
20. Rauf, A.; Kassas, M.; Khalid, M. Data-Driven Optimal Battery Storage Sizing for Grid-Connected Hybrid Distributed Generations Considering Solar and Wind Uncertainty. *Sustainability* **2022**, *14*, 11002. [CrossRef]
21. Kempton, W.; Letendre, S.E. Electric Vehicles as a New Power Source for Electric Utilities. *Transp. Res. Part D Transp. Environ.* **1997**, *2*, 157–175. [CrossRef]
22. Niu, Q.; Jiang, K.; Yang, Z. An Improved, Negatively Correlated Search for Solving the Unit Commitment Problem's Integration with Electric Vehicles. *Sustainability* **2019**, *11*, 6945. [CrossRef]

23. Growe-Kuska, N.; Heitsch, H.; Romisch, W. Scenario reduction and scenario tree construction for power management problems. In Proceedings of the 2003 IEEE Bologna Power Tech Conference Proceedings, Bologna, Italy, 23–26 June 2003; Volume 3, pp. 152–158. [CrossRef]
24. Ji, B.; Yuan, X.; Chen, Z.; Tian, H. Improved Gravitational Search Algorithm for Unit Commitment Considering Uncertainty of Wind Power. *Energy* **2014**, *67*, 52–62. [CrossRef]
25. Kennedy, J.; Eberhart, R. A discrete binary version of the particle swarm algorithm. In Proceedings of the 1997 IEEE International Conference on Systems, Man, and Cybernetics. Computational Cybernetics and Simulation, Orlando, FL, USA, 12–15 October 1997; Volume 5, pp. 4104–4108. [CrossRef]
26. Zhu, X.; Zhao, S.; Yang, Z.; Zhang, N.; Xu, X. A Parallel Meta-Heuristic Method for Solving Large Scale Unit Commitment Considering the Integration of New Energy Sectors. *Energy* **2022**, *238*, 121829. [CrossRef]
27. Dhaliwal, J.S.; Dhillon, J. A Synergy of Binary Differential Evolution and Binary Local Search Optimizer to Solve Multi-Objective Profit Based Unit Commitment Problem. *Appl. Soft Comput.* **2021**, *107*, 107387. [CrossRef]
28. Simopoulos, D.; Kavatza, S.; Vournas, C. Unit Commitment by an Enhanced Simulated Annealing Algorithm. *IEEE Trans. Power Syst.* **2006**, *21*, 68–76. [CrossRef]
29. Mirjalili, S.; Lewis, A. S-Shaped versus V-shaped Transfer Functions for Binary Particle Swarm Optimization. *Swarm Evol. Comput.* **2013**, *9*, 1–14. [CrossRef]
30. Gaing, Z.-L. Discrete particle swarm optimization algorithm for unit commitment. In Proceedings of the 2003 IEEE Power Engineering Society General Meeting (IEEE Cat. No. 03CH37491), Toronto, ON, Canada, 13–17 July 2003; pp. 418–424. [CrossRef]
31. Yang, Y.; Feng, Y.; Yang, L. Multi–Dimensional Firefly Algorithm Based on Local Search for Solving Unit Commitment Problem. *Front. Energy Res.* **2023**, *10*, 1005577. [CrossRef]
32. Jacob Raglend, I.; Veeravalli, S.; Sailaja, K.; Sudheera, B.; Kothari, D. Comparison of AI Techniques to Solve Combined Economic Emission Dispatch Problem with Line Flow Constraints. *Int. J. Electr. Power Energy Syst.* **2010**, *32*, 592–598. [CrossRef]
33. Venkatesh, P.; Gnanadass, R.; Padhy, N. Comparison and Application of Evolutionary Programming Techniques to Combined Economic Emission Dispatch with Line Flow Constraints. *IEEE Trans. Power Syst.* **2003**, *18*, 688–697. [CrossRef]
34. Venkatesh Kumar, C.; Ramesh Babu, M. An Exhaustive Solution of Power System Unit Commitment Problem Using Enhanced Binary Salp Swarm Optimization Algorithm. *J. Electr. Eng. Technol.* **2022**, *17*, 395–413. [CrossRef]
35. Xie, Y.G.; Chiang, H.D. A Novel Solution Methodology for Solving Large-scale Thermal Unit Commitment Problems. *Electr. Power Compon. Syst.* **2010**, *38*, 1615–1634. [CrossRef]
36. Dang, C.; Li, M. A Floating-Point Genetic Algorithm for Solving the Unit Commitment Problem. *Eur. J. Oper. Res.* **2007**, *181*, 1370–1395. [CrossRef]
37. Sun, L.; Zhang, Y.; Jiang, C. A Matrix Real-Coded Genetic Algorithm to the Unit Commitment Problem. *Electr. Power Syst. Res.* **2006**, *76*, 716–728. [CrossRef]
38. Jeong, Y.W.; Park, J.B.; Jang, S.H.; Lee, K.Y. A New Quantum-Inspired Binary PSO: Application to Unit Commitment Problems for Power Systems. *IEEE Trans. Power Syst.* **2010**, *25*, 1486–1495. [CrossRef]
39. Yuan, X.; Nie, H.; Su, A.; Wang, L.; Yuan, Y. An Improved Binary Particle Swarm Optimization for Unit Commitment Problem. *Expert Syst. Appl.* **2009**, *36*, 8049–8055. [CrossRef]
40. Shahid, M.; Malik, T.N.; Said, A. Heuristic Based Binary Grasshopper Optimization Algorithm to Solve Unit Commitment Problem. *Turk. J. Electr. Eng. Comput. Sci.* **2021**, *29*, 944–961. [CrossRef]
41. Pan, J.S.; Hu, P.; Chu, S.C. Binary Fish Migration Optimization for Solving Unit Commitment. *Energy* **2021**, *226*, 120329. [CrossRef]
42. Narimani, H.; Azizivahed, A.; Naderi, E.; Fathi, M.; Narimani, M.R. A Practical Approach for Reliability-Oriented Multi-Objective Unit Commitment Problem. *Appl. Soft Comput.* **2019**, *85*, 105786. [CrossRef]
43. Yuan-Kang, W.; Chih-Cheng, H.; Chun-Liang, L. Resolution of the Unit Commitment Problems by Using the Hybrid Taguchi-ant Colony System Algorithm. *Int. J. Electr. Power Energy Syst.* **2013**, *49*, 188–198. [CrossRef]